Synthesis and kinase inhibitory activity of new sulfonamide derivatives of pyrazolo[4,3-e][1,2,4]triazines

ARTICLE *in* EUROPEAN JOURNAL OF MEDICINAL CHEMISTRY · MARCH 2014

Impact Factor: 3.45 · DOI: 10.1016/j.ejmech.2014.03.054 · Source: PubMed

European Journal of Medicinal Chemistry 78 (2014) 217–224

Contents lists available at ScienceDirect

European Journal of Medicinal Chemistry

journal homepage: http://www.elsevier.com/locate/ejmech

Original article

Synthesis and kinase inhibitory activity of new sulfonamide derivatives of pyrazolo[4,3-*e*][1,2,4]triazines

Mariusz Mojzych [a,*,1], Veronika Šubertová [b,1], Anna Bielawska [c], Krzysztof Bielawski [c], Václav Bazgier [b], Karel Berka [d], Tomáš Gucký [b], Emilia Fornal [e], Vladimír Kryštof [b,*]

[a] *Department of Chemistry, Siedlce University of Natural Sciences and Humanities, ul. 3 Maja 54, Siedlce 08-110, Poland*
[b] *Centre of the Region Haná for Biotechnological and Agricultural Research, Laboratory of Growth Regulators, Faculty of Science, Palacký University, Šlechtitelů 11, 783 71 Olomouc, Czech Republic*
[c] *Department of Medicinal Chemistry and Drug Technology, Medical University of Bialystok, Bialystok, Poland*
[d] *Regional Centre of Advanced Technologies and Materials, Department of Physical Chemistry, Faculty of Science, Palacky University Olomouc, 17. listopadu 12, 77146 Olomouc, Czech Republic*
[e] *Department of Chemistry, Laboratory of Separation and Spectroscopic Method Applications, Center for Interdisciplinary Research, The John Paul II Catholic University of Lublin, al. Krasnicka 102, 20-718 Lublin, Poland*

ARTICLE INFO

Article history:
Received 2 December 2013
Received in revised form
13 March 2014
Accepted 16 March 2014
Available online 18 March 2014

Keywords:
Bcr-Abl
Kinase
Inhibitor
Synthesis
Cancer
Leukaemia
Pyrazolo[4,3-e][1,2,4]triazine

ABSTRACT

A new series of sulfonamide derivatives of pyrazolo[4,3-*e*][1,2,4]triazine has been synthesized and characterized. Their anticancer activity was tested *in vitro* against multiple human cancer cell lines and were found to have dose-dependent antiproliferative effects. Furthermore, some of the new compounds inhibited the Abl protein kinase with low micromolar IC_{50} values and exhibited selective activity against the Bcr-Abl positive K562 and BV173 cell lines, providing starting points for the further development of this new kinase inhibitor scaffold.

1. Introduction

Nitrogen-containing heterocycles have attracted huge interest over the past decades because of their diverse pharmacological activities, including protein kinase inhibition. Being involved in nearly all aspects of life at the cellular level, protein kinases have become the most important targets of drugs for various indications, such as cancers and inflammations [1–3]. Medicinal chemists have developed probes targeting a substantial fraction of the human kinome, and dozens of kinase inhibitors have been evaluated in clinical trials since the milestone approval of imatinib, the first anti-kinase drug targeting the fusion protein Bcr-Abl, a constitutively active tyrosine kinase that initiates the onset of chronic myelogenous leukaemia [4].

Despite the clear clinical success of imatinib, many tumours become resistant to it, often due to point mutations in the kinase domain of Bcr-Abl. Several second-generation drugs have been developed that inhibit some imatinib-resistant Bcr-Abl mutants, but there are still significant numbers of resistant mutants for which no alternative drugs are available [5]. The same may well be true for other pharmacologically relevant kinases. Consequently, there is still a need for new compounds that will enrich the pool of known inhibitors, especially if they possess novel scaffolds, binding modes or mechanisms of action.

Pyrazolo[4,3-*e*][1,2,4]triazine is a scaffold that has not yet received significant attention in drug discovery although some of its derivatives are known to exhibit biological activity. Over the last few decades, seven naturally occurring pyrazolo[4,3-*e*][1,2,4]triazines have been isolated and characterized spectroscopically and

* Corresponding authors.
E-mail address: vladimir.krystof@upol.cz (V. Kryštof).
[1] These authors contributed equally.

http://dx.doi.org/10.1016/j.ejmech.2014.03.054
0223-5234/

structurally: pseudoiodinine, nostocine A, and fluviols A–E [6–9]. In three cases, the proposed structures were verified by total synthesis [10]. Importantly, synthetic 1,3,5-substituted pyrazolo[4,3-*e*][1,2,4]triazines have been reported to exhibit significant activity against human cancer cell lines and to weakly inhibit cyclin-dependent kinase CDK2 [11].

The reported biological activities of pyrazolo[4,3-*e*][1,2,4]triazines might stem, at least in part, from their physicochemical similarity to purine, another nitrogen-containing heterocycle that is widely distributed in nature [12]. To date, chemical modification of the purine core (via scaffold hopping) has led to the discovery of various purine bioisosteres that have been used as scaffolds for the synthesis and development of chemical probes and drugs [12,13], including cyclin-dependent kinase (CDK) inhibitors [14]. The CDKs are a family of Ser/Thr kinases which, in association with specific cyclins, play critical roles as regulators of the different phases of the cell cycle. These enzymes and their direct regulators are frequently mutated, amplified, or deleted in malignant cells, suggesting that pharmacological CDK inhibition may be an effective strategy for treating cancer [14]. We have previously prepared and characterized many CDK inhibitors based on purine scaffolds [15–17] and bioisosteric alternatives such as 8-azapurines and pyrazolo[4,3-*d*]pyrimidines. Many of the compounds based on these bioisosteres are comparable or superior to the corresponding purine derivatives in terms of anticancer activity and kinase inhibition [18,19]. The discovery of kinase inhibitors based on new scaffolds is a major goal of our current research, and this prompted us to investigate the structure–activity relationships of pyrazolo[4,3-*e*][1,2,4]triazines. We have previously described the convenient synthesis and structural analysis of a series of 3,5,7-trisubstituted pyrazolo[4,3-*e*][1,2,4]triazines [20–22]. Herein we describe the synthesis and *in vitro* biological activity of sulfonamides with a pyrazolo[4,3-*e*][1,2,4]triazine core. The new compounds are shown to exhibit selective toxicity towards Bcr-Abl positive cells.

2. Results and discussion

2.1. Chemistry

The synthetic pathway leading to the title compounds is outlined in Scheme 1. Methylhydrazone **1**, the precursor of pyrazolo[4,3-*e*][1,2,4]triazine **2**, was prepared using a standard procedures. The cyclization of **1** to form **2** was then achieved under acidic conditions using a literature method [20,21]. Compound **2** was treated with potassium permanganate under phase transfer catalytic conditions at room temperature for 1 h to give sulfone **3** in nearly quantitative yield. Compound **3** was then reacted with anhydrous aniline in a sealed tube at 150 °C for 9 days. Chlorosulfonylation of the aniline-substituted pyrazolotriazine **4** in chlorosulfonic acid at 0 °C proceeded smoothly and selectively at the 4′-position of the phenyl ring to give the desired compound **5** in excellent yield. The chlorosulfonyl derivative **5** was readily coupled with amines to produce the target sulfonamides **6a**–**l** as shown in Scheme 1.

The structures and purity of the newly synthesized compounds were characterized using ^{1}H and ^{13}C NMR spectroscopy, HPLC-MS, and elemental analysis. The spectral data confirmed that all of the new sulfonamides had the expected structures and were of high purity.

2.2. Antiproliferative activity in vitro

The antiproliferative activity of the new compounds against several breast carcinoma (MCF-7, MDA-MB-231) and leukaemia

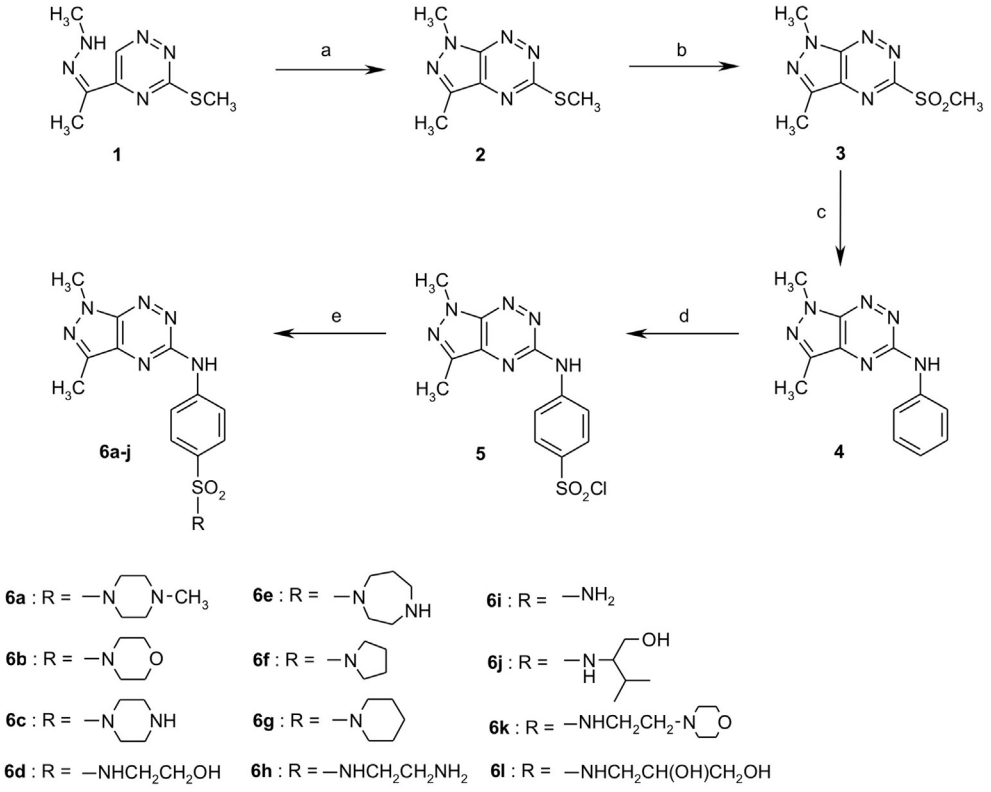

Scheme 1. Reagents and conditions: (a) p-TSA, T; (b) $KMnO_4$, Bu_4NBr, CH_3COOH, benzene-H_2O, rt, 2 h; (c) aniline, seal tube, 9 days, 150 °C; (d) $ClSO_3H$, 0 °C to rt, 2 h; (e) NH_3 or amine, MeCN, rt.

(K562, BV173, HL60, CCRF-CEM) cell lines was measured using the MTT assay after 24 h of incubation [23]. The results obtained are summarized in Table 1. Concentration-dependent activity was observed in all cases. The breast carcinoma lines were much less sensitive to all of the compounds (with IC_{50} values ranging from 100 to 200 μM) than the leukaemia cell lines. However, in general, the compounds had similar rankings with respect to activity in all cell lines, with the most active being **6a**, **6c**, **6e** and **6h**. All of these species have similar side chains (*N*-methylpiperazine, piperazine, homopiperazine, 1,2-diaminoethane). Conversely, compounds **6d**, **6f**, **6i**, and **6j** exhibited very little activity.

The IC_{50} values for the tested leukaemia cell lines ranged from 20 to 70 μM for CCRF-CEM, 24 to 58 μM for HL60, and 27 to 72 μM for BV173. The IC_{50} range for the K562 line was even broader, with the most potent compound **6e** having a value of 21 μM while **6j** was inactive even at 200 μM. Surprisingly, the IC_{50} values for the most potent compounds against K562 – **6e** and **6c** – were 7 and 5 times lower than their IC_{50} values against breast carcinoma cell lines, respectively. This suggests that these compounds exhibit a degree of selective toxicity towards the K562 cell line. A similar activity pattern was observed in the BV173 cell line, with the most potent compounds again being **6e** and **6c**.

The compounds' antiproliferative activities are probably at least partly due to their cytostatic effects: preliminary investigations using breast carcinoma cell lines showed that they prevent the incorporation of [^{3}H]thymidine into living cells. As in the MTT assay, all of the tested compounds exhibited concentration-dependent activity with different potencies (Supplementary Table S1). However, cytostatic effects alone cannot fully explain their antiproliferative activity because in several cases, the number of viable cells declined significantly after as little as 24 h of treatment. We therefore investigated the influence of the most potent compounds (**6c**, **6e** and **6h**) on the viability of K562 cells using the propidium iodide exclusion assay. Treatment with compound **6c** or **6e** caused sharp increases in the number of cells with compromised cell membranes (Fig. 1a). In parallel, we evaluated the test compounds' effects on cell cycling and found that **6c** and **6e** had no effect on the distribution of cell cycle phases (data not shown) but did cause pronounced increases in the sub-diploid population, which is indicative of ongoing apoptotic cell death (Fig. 1b). Compound **6h** had only marginal effects on viability and did not increase the sub-diploid cell population.

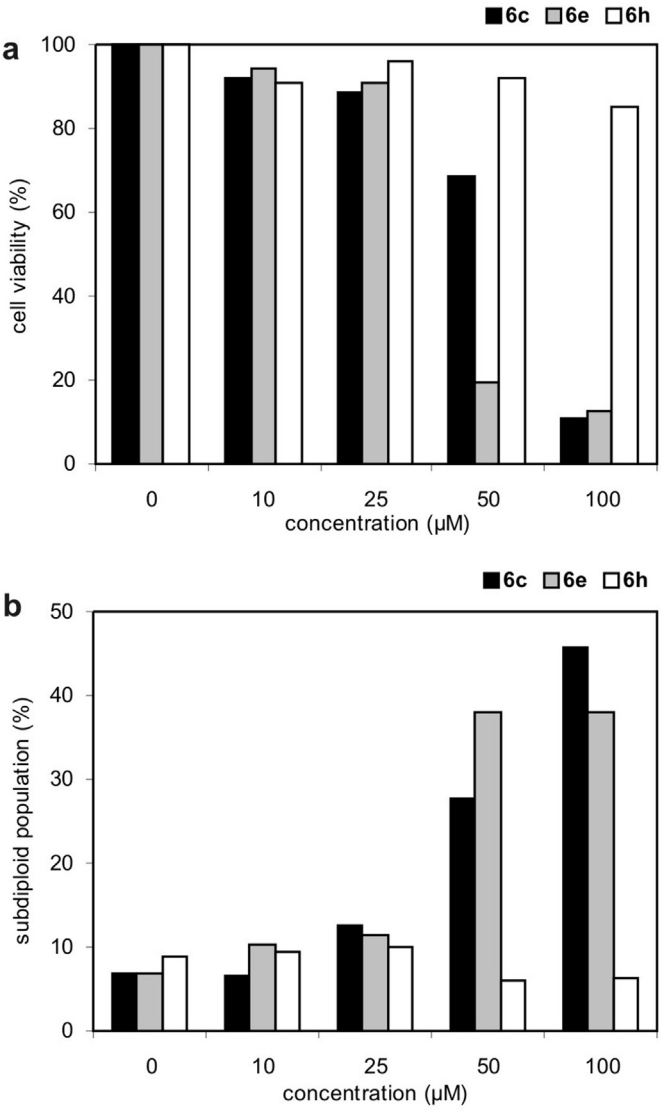

Fig. 1. Effect of test compounds on K562 cell viability after 24 h treatment. Propidium iodide exclusion (**a**) and the sub-diploid cell population (**b**) were quantified by flow cytometry in native or in ethanol-fixed cells, respectively.

Table 1
In vitro antiproliferative activity of new sulfonamide derivatives of pyrazolo[4,3-e]-[1,2,4]triazine after 24 h incubation.

Compd.	MTT assay, IC_{50} (μM)[a]					
	MCF-7	MDA-MB-231	K562	BV173	HL60	CCRF-CEM
6a	102 ± 2	99 ± 2	66 ± 5	40 ± 8	49 ± 2	36 ± 2
6b	>200	>200	90 ± 8	58 ± 5	39 ± 1	69 ± 8
6c	150 ± 2	130 ± 2	27 ± 4	22 ± 6	55 ± 2	20 ± 2
6d	>200	>200	100 ± 4	41 ± 10	42 ± 5	49 ± 8
6e	140 ± 3	155 ± 2	21 ± 5	22 ± 4	38 ± 1	36 ± 12
6f	>200	>200	102 ± 1	47 ± 14	56 ± 6	30 ± 2
6g	200 ± 2	140 ± 1	98 ± 2	36 ± 9	24 ± 2	30 ± 2
6h	126 ± 1	120 ± 1	77 ± 7	39 ± 8	42 ± 6	56 ± 2
6i	>200	>200	106 ± 8	45 ± 11	58 ± 3	50 ± 1
6j	>200	>200	>200	58 ± 9	40 ± 2	54 ± 8
6k	146 ± 1	125 ± 2	96 ± 3	39 ± 8	41 ± 1	64 ± 6
6l	200 ± 2	140 ± 2	101 ± 2	42 ± 9	44 ± 5	57 ± 3
Chlorambucil	97 ± 2	93 ± 2	84 ± 6	34 ± 8	38 ± 2	21 ± 8
Imatinib	n.a.	n.a.	13 ± 2	20 ± 6	55 ± 7	45 ± 1

[a] The reported values represent the mean ± S.D. for each compound based on four independent experiments.

2.3. Kinase inhibitory activity

The enhanced potency of the new pyrazolo[4,3-*e*][1,2,4]triazines against the K562 and BV173 cell lines (both of which are Bcr-Abl positive) relative to other cell lines prompted us to explore their inhibitory potency against a purified recombinant Abl kinase. The seven tested compounds significantly inhibited Abl activity, with IC_{50} values in the micromolar range (Table 2). The most potent compounds **6c** and **6e** bear piperazine (IC_{50} values of 5.8 μM) and homopiperazine (IC_{50} values of 5.9 μM) appendages, respectively. Such rings, and especially the secondary amines within them, seem to be important for Abl inhibition: analogues bearing a methyl-substituted piperazine (**6a**) or deaza and oxo analogues (piperidine and morpholine derivatives **6g** and **6b**, respectively) exhibited dramatically lower activity (Table 2 and supplementary table S2). The acyclic 2-aminoethylamine derivative **6h** also exhibited somewhat lower activity (IC_{50} = 15 μM). All other derivatives were either much weaker inhibitors (unsubstituted sulfonamide **6i** and hydroxyalkyl sulfonamides **6d** and **6l**) or entirely inactive at the tested concentrations (**6j** and **6f**).

Table 2
Inhibition of protein kinases by sulfonamide derivatives of pyrazolo[4,3-*e*][1,2,4]triazines.

Compd.	IC_{50} (μM)		
	Abl	CDK2	CK2
6a	>50	>50	>50
6b	>25	>25	>25
6c	5.8	>25	>25
6d	39	>50	>50
6e	5.9	>50	>50
6f	>50	>50	>50
6g	>25	>25	>25
6h	15.0	34.9	>50
6i	33.0	>50	>50
6j	>50	>50	>50
6k	20	>50	>50
6l	34.0	>50	>50
Roscovitine	>100	0.1	n.a.
Imatinib	0.3	>100	n.a.
Silmitasertib	n.a.	1.8	0.1

To better understand the molecular basis for the inhibitory activity of the pyrazolo[4,3-*e*][1,2,4]triazine derivatives, we used molecular modelling to rationalize their binding to Abl. We hypothesized that compounds **6c** and **6e** might bind to the ATP-binding site of the Abl kinase in a manner similar to that of pyrido[2,3-d]pyrimidine PD180970, interacting with the protein primarily via non-polar interactions and H-bonds with the backbone NH group of the M318 residue [24]. Our studies confirmed that both **6c** and **6e** dock into the Abl kinase in this way. The piperazine ring of **6c** fits in to a pocket of the active site that is lined by the gatekeeper residue T315. This is the pocket occupied by the dichlorophenyl group of PD180970 and the methylbenzene moiety of imatinib. In addition, we observed a possible H-bond between I313 and the secondary amino groups on the sulfonamide appendages of **6c** and **6e** (Fig. 2). This H-bond has not previously been observed in any Abl co-crystal structure but its presence is consistent with the SAR data presented above: the analogous 2-aminoethylamine derivative **6h** is less active despite having a primary amine at about the right distance from I313 to form a similar H-bond, probably due to the greater flexibility of its side chain. The same is true for the even less active hydroxy derivative **6d**. The inactivity of compounds that lack a secondary amine or other H-bond acceptor capable of forming an interaction of this sort (*e.g.* the methyl-substituted compound **6a**, piperidine **6g**, and morpholine **6b**) further supports this hypothesis.

2.4. Kinase inhibition selectivity

We have recently demonstrated that certain pyrazolo[4,3-*e*][1,2,4]triazines inhibit CDK2/cyclin E [22]. However, most of the compounds synthesized in this work did not inhibit either CDK2 or CK2 within the tested concentration range, showing that they have some degree of selectivity for Abl (Table 2). The only exception is compound **6h**, which exhibited weak activity towards CDK2 (IC_{50} = 34.9 μM). This may contribute to its marginal antiproliferative effects (Table 1). These preliminary selectivity data are however not sufficient to exclude the possibility that the new compounds may bind to and inhibit other targets, including other protein kinases.

To clarify the new compounds' lack of activity towards CDK2 and guide future optimization, we investigated the interactions of the pyrazolo[4,3-*e*][1,2,4]triazine derivatives with CDK2. Molecular docking experiments suggested that the mostly negative results obtained in the biochemical assays are due to the relatively unfavourable mode of binding adopted by the pyrazolo[4,3-*e*][1,2,4]triazines in the CDK2 active site (Fig. 3). Well-known purine CDK inhibitors such as olomoucine and roscovitine typically bear small hydrophobic chain at N9, an aromatic ring attached to the secondary amino group at C6, and a polar alkyl amine at C2. In addition, they have no substituents at N7 [13,14,16]. This substitution pattern, together with the donor–acceptor H-bond motif formed by the N7 group and the secondary amino group at C6 that interacts with the hinge region of CDK2, gives the known CDK2 inhibitors a well-defined binding orientation within the CDK2 active site. Because pyrazolo[4,3-*e*][1,2,4]triazines cannot be substituted at the corresponding positions, we anticipated, based on the well known structure–activity relationships for CDK inhibitors [15–17], that they might instead bind to CDK2 in a 'reversed' orientation, similar to that adopted by the guanine-based inhibitor NU6102 [25]. NU6102 binds to the hinge region via H-bonds involving the secondary amino group at C2 and purine nitrogens N3 and N9 (Fig. 3). However, it is likely that the methyl substitution of the pyrazole ring would both abolish one of these H-bonds and also form an unfavourable steric interaction that would discourage the binding of **6h** in the active site (Fig. 3a).

2.5. Cellular inhibition of tyrosine kinases

Compounds **6c** and **6e** emerged as most potent Abl inhibitors from this series. Because of their strong antiproliferative activity in Bcr-Abl positive cell lines (K562 and BV173), we decided to characterize their cellular effects in more detail. Derivative **6h** was also included in these experiments due to its lower activity and broader selectivity. We treated K652 cells with increasing doses of **6c**, **6e** and **6h** for 1 h and immunoblotted the cell lysates with phospho-specific antibodies towards phosphorylated forms of STAT5 and CrkL, known substrates of Bcr-Abl kinase that both contribute to the sustained proliferation of leukaemic cells (Fig. 4a). All three

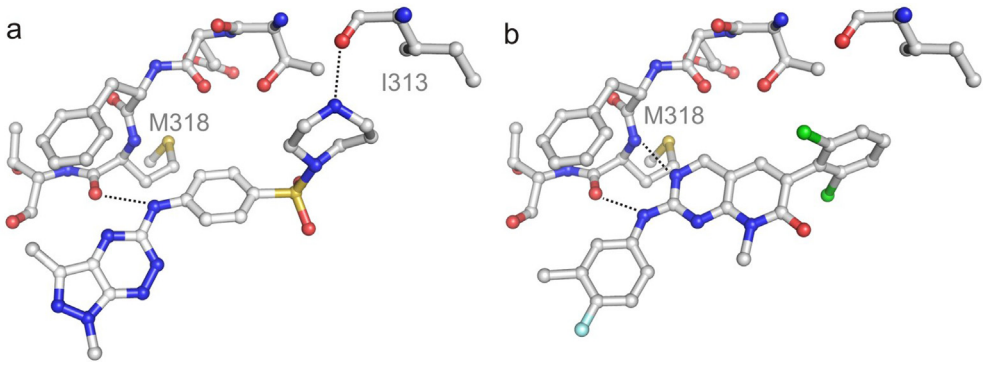

Fig. 2. The binding poses of compound **6e** (**a**) and PD180970 (**b**) in c-Abl (PDBID: 2hzi). The compounds' interactions with I313 and M318 are indicated by dotted lines.

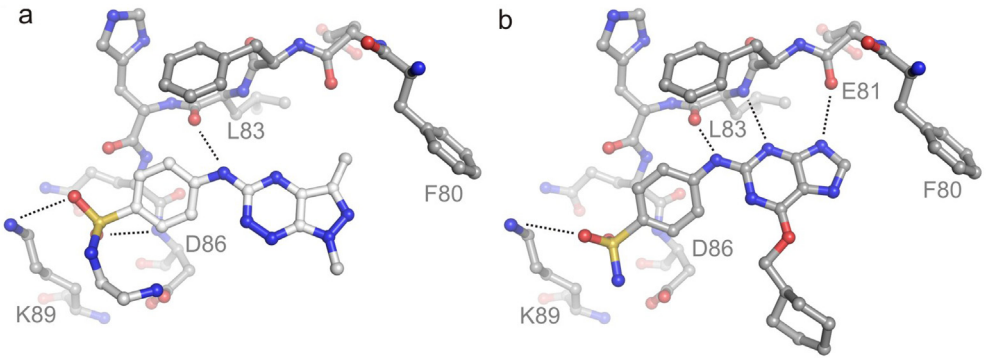

Fig. 3. The binding poses of compound **6h** (**a**) and NU6102 (**b**) in CDK2 (PDBID: 2c60). Interactions with D86, K89 and with the backbone of L83 and E81 are indicated by dotted lines.

derivatives caused dose–response decreases in the phosphorylation of STAT5, but only **6c** reduced the phosphorylation of CrkL.

We also evaluated the influence of the most potent compounds on the global tyrosine phosphorylation status of the proteins in K562 cells. This was done by immunoblotting their lysates with an anti-phosphotyrosine antibody (Fig. 4b). In untreated cells, several proteins phosphorylated on tyrosine residues were detected. Treatment with derivatives **6c** and **6e** reduced the phosphorylation of some of these proteins in a dose-dependent manner, including some that formed intense bands with molecular weights between 150 and 250 kDa and probably corresponded to Abl and Bcr-Abl [26]. In addition, at least three additional phosphoproteins with molecular weights between 40 and 60 kDa (which yielded weaker bands) exhibited dose-dependent reductions in signal intensity. Importantly, treatment with the less active derivative **6h** did not reduce the phosphorylation of any of these proteins whereas imatinib (which was used as a positive control in both experiments) rapidly inhibited the phosphorylation of several proteins.

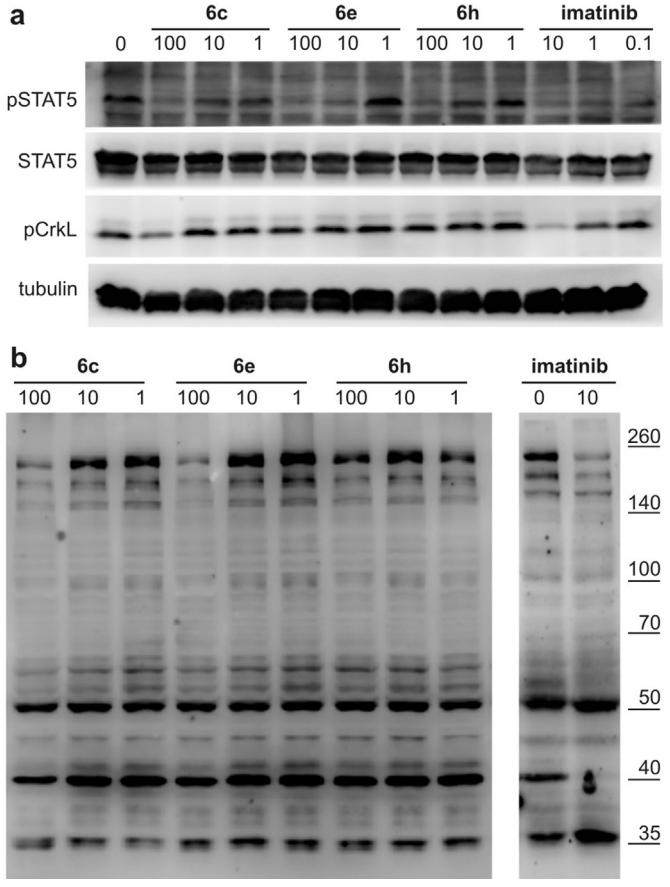

Fig. 4. Phosphoprotein analysis of K562 cells treated with test compounds. The cells were incubated for 1 h with the indicated doses of **6c**, **6e** and **6h** (in μM), lysed and immunoblotted with anti-phospho-STAT5, anti-STAT5, anti-phospho-CrkL and anti-tubulin antibodies (**a**). In a second experiment, the immunoblotting was performed with an anti-phosphotyrosine antibody (**b**). Imatinib (0.1, 1 or 10 μM) was used as a positive control in both experiments.

3. Conclusions

We have described an efficient method for the preparation of sulfonamide derivatives of pyrazolo[4,3-*e*][1,2,4]triazines (**6**). Approximately half of the prepared compounds exhibited modest activity towards cancer cell lines. In addition, our study identified two compounds, **6c** and **6e**, that exhibit micromolar inhibition of the Abl protein kinase and preferential antiproliferative activity in leukaemia cell lines that overexpress the oncogenic kinase Bcr-Abl. These compounds represent new scaffolds for protein kinase inhibitors, which are still needed in oncological drug discovery, especially because of the emerging resistance to existing drugs. Further studies aimed at optimizing the structures of the hits in order to increase their potency against the Bcr-Abl kinase and cancer cell lines *in vitro* are currently underway in our laboratories.

4. Experimental section

4.1. Chemistry

Melting points were determined on a Mel-Temp apparatus and are uncorrected. ^{1}H and ^{13}C NMR spectra were recorded on a Varian spectrometer (400 and 100 MHz, respectively). Chemical shift values are expressed in ppm (part per million) relative to tetramethylsilane as an internal standard. The relative integrals of peak areas agreed with those expected for the assigned structures. The molecular weights of the final compounds were determined by electrospray ionization mass spectrometry (ESI/MS) performed using an Agilent Technologies 6538 UHD Accurate Mass Q-TOF LC/MS. All elemental compositions were within ±0.4% of the calculated values.

4.2. Synthesis of precursors

4.2.1. 1,3-Dimethyl-5-phenylamino-1H-pyrazolo[4,3-e][1,2,4] triazine (*4*)

A mixture of **3** (1.68 g, 7.37 mmol) and freshly distilled aniline (10 ml, 110 mmol) was introduced into **a** sealed tube and heated at

150 °C for 9 days. The excess aniline was then distilled out from the reaction mixture, and the resulting residue was purified by column chromatography on silica gel, eluting with a mixture of ethyl acetate/hexane (1:1). The combined fractions were evaporated, providing the crude product **4** as an orange solid (0.74 g, 3.07 mmol). Yield 42%, mp 215–217 °C. ^{1}H NMR (DMSO-d_6) δ: 2.49 (s, 3H), 4.09 (s, 3H), 6.98 (t, 1H, J = 7.6 Hz), 7.32 (t, 2H, J = 7.4 Hz), 7.81 (d, 2H, J = 9.0 Hz), 10.26 (s, 1H, NH). ^{13}C NMR (DMSO-d_6) δ: 10.72, 34.67, 118.54, 121.93, 128.95, 133.05, 138.33, 140.42, 146.17, 158.36. HRMS (ESI, *m*/*z*) calcd. for $C_{12}H_{13}N_6$ [M+H] 241.1196. Found 241.1195. Anal. Calcd. for $C_{12}H_{12}N_6$: C, 59.99; H, 5.03; N, 34.98. Found: C, 59.76; H, 5.06; N, 34.84.

4.2.2. 4-(1,3-Dimethyl-1H-pyrazolo[4,3-e][1,2,4]triazin-5-ylamino) benzene-1-sulfonyl chloride (5)

Compound **4** (1.03 g, 4.28 mmol) was added portionwise to stirred and ice-cooled chlorosulfonic acid (9.03 g, 77.48 mmol) under an argon atmosphere, after which the reaction mixture was gradually warmed to room temperature over 2 h. The reaction solution was cautiously poured over crushed ice (40 g) and the aqueous mixture was extracted with dichloromethane. The combined extracts were dried over anhydrous Na_2SO_4 and evaporated under reduced pressure to give the required sulfonyl chloride **5** as a yellow solid (1.37 g, 4.03 mmol). Yield 94%, mp 233 °C. ^{1}H NMR (DMSO-d_6) δ: 2.49 (s, 3H), 4.10 (s, 3H), 7.57 (d, 2H, J = 8.4 Hz), 7.79 (d, 2H, J = 8.8 Hz), 10.43 (s, 1H, NH). ^{13}C NMR (DMSO-d_6) δ: 10.56, 34.52, 117.17, 126.25, 132.86, 138.17, 140.69, 140.78, 146.04, 157.95.

4.3. General procedure for preparation of the sulfonamides (**6a**–**l**)

A mixture of chlorosulfonyl derivative (**5**) (100 mg, 0.29 mmol) and the appropriate amine (1.00 mmol) in anhydrous acetonitrile (10 ml) was stirred overnight at room temperature, after which the reaction mixture was concentrated under reduced pressure to afford crude sulfonamides, **6a**–**l** as yellow solids. The residues were purified by crystallization from EtOH or by column chromatography on silica using a mixture of CH_2Cl_2:EtOH (25/1, v/v) as the eluent.

4.3.1. 1,3-Dimethyl-N-[4-(4-methylpiperazin-1-ylsulfonyl)phenyl]-1H-pyrazolo[4,3-e][1,2,4]triazin-5-amine (**6a**)

Yield 71%, mp 246–251 °C. ^{1}H NMR ($CDCl_3$) δ: 2.27 (s, 3H), 2.50–2.52 (m, 4H), 2.63 (s, 3H), 3.07–3.08 (m, 4H), 4.25 (s, 3H), 7.77 (d, 2H, J = 8.8 Hz), 7.93 (d, 2H, J = 8.8 Hz), 8.12 (s, 1H, NH). ^{13}C NMR ($CDCl_3$) δ: 10.87, 34.80, 45.68, 45.95, 54.07, 117.62, 127.98, 129.36, 133.97, 139.76, 143.53, 146.64, 157.14. HRMS (ESI, *m*/*z*) calcd. for $C_{17}H_{23}N_8O_2S$ [M+H] 403.1659. Found 403.1661. Anal. Calcd. for $C_{17}H_{22}N_8O_2S$: C, 50.73; H, 5.51; N, 27.84. Found: C, 50.50; H, 5.53; N, 27.71.

4.3.2. 1,3-Dimethyl-N-(4-(morpholinosulfonyl)phenyl)-1H-pyrazolo[4,3-e][1,2,4]triazin-5-amine (**6b**)

Yield 72%, mp 280–285 °C. ^{1}H NMR ($CDCl_3$) δ: 2.64 (s, 3H), 3.03 (t, 4H, J = 4.8 Hz), 3.76 (t, 4H, J = 4.8 Hz), 4.26 (s, 3H), 7.77 (d, 2H, J = 6.8 Hz), 7.97 (d, 2H, J = 6.8 Hz), 8.19 (s, 1H, NH). ^{13}C NMR ($CDCl_3$) δ: 10.87, 34.81, 46.05, 66.13, 117.65, 127.66, 129.43, 133.39, 139.75, 143.75, 146.65, 157.12. HRMS (ESI, *m*/*z*) calcd. for $C_{16}H_{20}N_7O_3S$ [M+H] 390.1343. Found 390.1342. Anal. Calcd for $C_{16}H_{19}N_7O_3S$: C, 49.35; H, 4.92; N, 25.18. Found: C, 49.09; H, 4.95; N, 25.04.

4.3.3. 1,3-Dimethyl-N-[4-(piperazin-1-ylsulfonyl)phenyl]-1H-pyrazolo[4,3-e][1,2,4]triazin-5-amine (**6c**)

Yield 86%, mp 300–307 °C. ^{1}H NMR (DMSO-d_6) δ: 2.52 (s, 3H), 2.79–2.81 (m, 8H), 4.15 (s, 3H), 7.68 (d, 2H, J = 8.8 Hz), 8.09 (d, 2H, J = 8.8 Hz), 10.92 (s, 1H, NH). ^{13}C NMR (DMSO-d_6) δ: 10.54, 34.56, 44.27, 46.14, 117.45, 126.04, 128.94, 132.78, 138.47, 144.76, 146.18, 157.32. HRMS (ESI, *m*/*z*) calc. for $C_{16}H_{21}N_8O_2S$ [M+H] 389.1503. Found 389.1502. Anal. Calcd for $C_{16}H_{20}N_8O_2S$: C, 49.47; H, 5.19; N, 28.85. Found: C, 49.17; H, 5.23; N, 28.67.

4.3.4. 4-(1,3-Dimethyl-1H-pyrazolo[4,3-e][1,2,4]triazin-5-ylamino)-N-(2-hydroxyethyl)-benzenesulfonamide (**6d**)

Yield 65%, mp 242–244 °C. ^{1}H NMR (DMSO-d_6) δ: 2.53 (s, 3H), 2.78 (t, 2H, J = 6.0 Hz), 3.36 (q, 2H, J = 6.0 Hz), 4.16 (s, 3H), 4.64 (t, 1H, J = 6.0 Hz, OH), 7.37 (bs, 1H, NH), 7.75 (d, 2H, J = 8.4 Hz), 8.02 (d, 2H, J = 8.4 Hz), 10.82 (bs, 1H, NH). ^{13}C NMR (DMSO-d_6) δ: 10.53, 34.52, 45.10, 59.93, 117.45, 127.72, 132.26, 132.73, 138.38, 143.88, 146.08, 157.39. HRMS (ESI, *m*/*z*) calcd. for $C_{14}H_{18}N_7O_3S$ [M+H] 364.1186. Found 364.1186. Anal. Calcd. for $C_{14}H_{17}N_7O_3S$: C, 46.27; H, 4.72; N, 26.98. Found: C, 46.04; H, 4.74; N, 26.84.

4.3.5. N-[4-(1,4-Diazepan-1-ylsulfonyl)phenyl]-1,3-dimethyl-1H-pyrazolo[4,3-e][1,2,4]triazin-5-amine (**6e**)

Yield 70%, mp 168–174 °C. ^{1}H NMR (DMSO-d_6) δ: 1.76–1.80 (m, 2H), 2.52 (s, 3H), 2.72 (t, 2H, J = 12.0 Hz), 2.77 (t, 2H, J = 10.0 Hz), 3.20 (t, 2H, J = 10.0 Hz), 3.25 (t, 2H, J = 12.0 Hz), 4.15 (s, 3H), 4.18 (bs, 1H, NH), 7.73 (d, 2H, J = 8.8 Hz), 8.05 (d, 2H, J = 8.8 Hz), 10.92 (bs, 1H, NH). ^{13}C NMR (DMSO-d_6) δ: 10.50, 27.87, 34.51, 45.74, 46.82, 47.89, 48.10, 117.52, 128.02, 129.89, 132.67, 138.36, 144.36, 146.07, 157.29. HRMS (ESI, *m*/*z*) calc. for $C_{17}H_{23}N_8O_2S$ [M+H] 403.1659. Found 403.1660. Anal. Calcd. for $C_{17}H_{22}N_8O_2S$: C, 50.73; H, 5.51; N, 27.84. Found: C, 50.52; H, 5.53; N, 27.72.

4.3.6. 1,3-Dimethyl-N-[4-(pyrrolidin-1-ylsulfonyl)phenyl]-1H-pyrazolo[4,3-e][1,2,4]triazin-5-amine (**6f**)

Yield 88%, mp 284–286 °C. ^{1}H NMR (DMSO-d_6) δ: 1.63–1.66 (m, 4H), 2.52 (s, 3H), 3.12–3.15 (m, 4H), 4.15 (s, 3H), 7.76 (d, 2H, J = 8.8 Hz), 8.07 (d, 2H, J = 8.8 Hz), 10.88 (s, 1H, NH). ^{13}C NMR (DMSO-d_6) δ: 10.67, 24.67, 34.65, 47.79, 117.40, 127.61, 128.54, 132.70, 138.39, 144.47, 146.10, 157.33. HRMS (ESI, *m*/*z*) calcd. for $C_{16}H_{20}N_7O_2S$ [M+H] 374.1394. Found 374.1396. Anal. Calcd. for $C_{16}H_{19}N_7O_2S$: C, 51.46; H, 5.13; N, 26.26. Found: C, 51.30; H, 5.15; N, 26.19.

4.3.7. 1,3-Dimethyl-N-[4-(piperidin-1-ylsulfonyl)phenyl]-1H-pyrazolo[4,3-e][1,2,4]triazin-5-amine (**6g**)

Yield 85%, mp 241–248 °C. ^{1}H NMR (DMSO-d_6) δ: 1.29–1.38 (m, 2H), 1.60–1.66 (m, 4H), 2.53 (s, 3H), 2.95–2.98 (m, 4H), 4.13 (s, 3H), 7.66 (d, 2H, J = 8.4 Hz), 8.06 (d, 2H, J = 8.4 Hz), 10.89 (bs, 1H, NH). ^{13}C NMR (DMSO-d_6) δ: 10.70, 22.12, 24.70, 43.54, 46.66, 117.43, 126.80, 128.61, 132.70, 138.41, 144.53, 146.11, 157.32. HRMS (ESI, *m*/*z*) calcd. for $C_{17}H_{22}N_7O_2S$ [M+H] 388.1550. Found 388.1510. Anal. Calcd for $C_{17}H_{21}N_7O_2S$: C, 52.70; H, 5.46; N, 25.31. Found: C, 52.45; H, 5.49; N, 25.18.

4.3.8. N-(2-Aminoethyl)-4-(1,3-dimethyl-1H-pyrazolo[4,3-e][1,2,4] triazin-5-ylamino)benzenesulfonamide (**6h**)

Yield 78%, mp 238–242 °C. ^{1}H NMR (DMSO-d_6) δ: 2.51 (s, 3H), 2.65 (t, 2H, J = 6.6 Hz), 2.82 (t, 2H, J = 6.4 Hz), 4.08 (bs, 2H, NH_2), 4.14 (s, 3H), 7.75 (d, 2H, J = 8.8 Hz), 8.03 (d, 2H, J = 8.8 Hz), 10.86 (bs, 1H, NH). ^{13}C NMR (DMSO-d_6) δ: 10.53, 34.53, 43.30, 117.48, 127.79, 131.76, 132.78, 138.39, 144.03, 146.14, 157.38. HRMS (ESI, *m*/*z*) calcd. for $C_{14}H_{19}N_8O_2S$ [M+H] 363.1346. Found 363.1346. Anal. Calcd. for $C_{14}H_{18}N_8O_2S$: C, 46.40; H, 5.01; N, 30.92. Found: C, 46.20; H, 5.03; N, 30.81.

4.3.9. 4-(1,3-Dimethyl-1H-pyrazolo[4,3-e][1,2,4]triazin-5-ylamino) benzenesulfonamide (**6i**)

Yield 82%, mp 317–320 °C. ^{1}H NMR (DMSO-d_6) δ: 2.49 (s, 3H), 4.12 (s, 3H), 7.18 (s, 2H, NH_2), 7.76 (d, 2H, J = 8.4 Hz), 7.96 (d, 2H, J = 8.4 Hz), 10.74 (s, 1H, NH). ^{13}C NMR (DMSO-d_6) δ: 10.66, 34.65,

117.55, 126.87, 132.95, 136.38, 138.55, 143.52, 146.24, 157.60. HRMS (ESI, *m*/*z*) calcd. for $C_{12}H_{14}N_7O_2S$ [M+H] 320.0924. Found 320.0923. Anal. Calcd. for $C_{12}H_{13}N_7O_2S$: C, 45.13; H, 4.10; N, 30.70. Found: C, 44.83; H, 4.16; N, 30.53.

4.3.10. 4-(1,3-Dimethyl-1H-pyrazolo[4,3-e][1,2,4]triazin-5-ylamino)-N-(1-hydroxy-3-methylbutan-2-yl)benzenesulfonamide (**6j**)

Yield 75%, mp 306–307 °C. ^{1}H NMR (DMSO-d_6) δ: 0.71 (d, 3H, J = 6.8 Hz), 0.75 (d, 3H, J = 6.8 Hz), 1.80–1.86 (m, 1H), 2.53 (s, 3H), 2.87–2.91 (m, 1H), 3.10–3.17 (m, 2H), 4.15 (s, 3H), 4.49 (t, 1H, J = 5.4 Hz, OH), 7.14 (d, 1H, J = 8.4 Hz, NH), 7.75 (d, 2H, J = 9.2 Hz), 8.01 (d, 2H, J = 9.2 Hz), 10.84 (bs, 1H, HN). HRMS (ESI, *m*/*z*) calcd. for $C_{17}H_{24}N_7O_3S$ [M+H] 406.1656. Found 406.1655. Anal. Calcd for $C_{17}H_{23}N_7O_3S$: C, 50.36; H, 5.72; N, 24.18. Found: C, 50.09; H, 5.74; N, 24.07.

4.3.11. (1,3-Dimethyl-1H-pyrazolo[4,3-e][1,2,4]triazin-5-ylamino)-N-(2-morpholinoethyl)-benzenesulfonamide (**6k**)

Yield 76%, mp 218–220 °C. ^{1}H NMR (DMSO-d_6) δ: 2.26–2.31 (m, 6H), 2.49 (s, 3H), 2.84 (q, 2H, J = 6.4 Hz), 3.49 (t, 4H, J = 4.4 Hz), 4.13 (s, 3H), 7.29 (t, 2H, J = 5.2 Hz), 7.74–7.76 (d, 2H, J = 8.8 Hz), 8.00 (d, 2H, J = 8.8 Hz), 10.79 (s, 1H, NH). ^{13}C NMR (DMSO-d_6) δ: 10.51, 15.25, 34.52, 53.05, 57.09, 65.97, 117.44, 127.73, 131.76, 132.78, 138.36, 144.03, 146.14, 157.39. HRMS (ESI, *m*/*z*) calcd. for $C_{18}H_{25}N_8O_3S$ [M+H] 433.1765. Found 433.1763. Anal. Calcd. for $C_{18}H_{24}N_8O_3S$: C, 49.99; H, 5.59; N, 25.91. Found: C, 49.75; H, 5.62; N, 25.74.

4.3.12. N-(2,3-Dihydroxypropyl)-4-(1,3-dimethyl-1H-pyrazolo[4,3-e][1,2,4]triazin-5-ylamino)-benzenesulfonamide (**6l**)

Yield 87%, mp 235–236 °C. ^{1}H NMR (DMSO-d_6) δ: 2.50 (s, 3H), 2.60 (dd, 1H, J_1 = 7.2 Hz, J_2 = 1.32 Hz), 2.85 (dd, 1H, J_1 = 5.2 Hz, J_2 = 1.28 Hz), 3.24–3.28 (m, 2H), 3.42–3.50 (m, 1H). 4.13 (s, 3H), 4.45 (t, 1H, J = 3.6 Hz, OH), 4.70 (d, 1H, J = 4.4 Hz, OH), 7.23 (bs, 1H, NH), 7.74 (d, 2H, J = 8.4 Hz), 8.00 (d, 2H, J = 8.4 Hz), 10.80 (bs, 1H, NH). ^{13}C NMR (DMSO-d_6) δ: 10.52, 34.51, 46.05, 63.52, 70.30, 117.40, 127.74, 132.15, 132.75, 138.37, 143.83, 146.11, 157.40. HRMS (ESI, *m*/*z*) calcd. for $C_{15}H_{19}N_7O_4S$ [M+H] 394.1292. Found 394.1292. Anal. Calcd. for $C_{15}H_{19}N_7O_4S$: C, 45.79; H, 4.87; N, 24.92. Found: C, 45.52; H, 5.03; N, 24.79.

4.4. Cell cultures

Human cancer cell lines MCF-7, MDA-MB-231, K562, CCRF-CEM, HL60 and BV173 (purchased from the American Type Culture Collection and the German Collection of Microorganisms and Cell Cultures) were maintained in DMEM supplemented with 10% foetal bovine serum (FBS), 50 U/ml penicillin, 50 μg/ml streptomycin at 37 °C. Cells were cultured in Costar flasks and subconfluent cells were detached with trypsin (in case of breast cell lines), counted and plated at 5×10^5 cells per well in 6-well plates (Nunc) in 2 ml of growth medium. Cells reached 80% confluency on day 3 and in most cases such cells were used for the assays.

4.5. MTT assay

The assay was performed according to the literature method [23]. Cells exposed for 24 h to various concentrations of the studied compounds in microtitre plates were stained with MTT solution at 37 °C. The solution was then removed and 1 ml of 0.1 M HCl in absolute isopropanol was added to the attached cells. The absorbance of the converted dye in living cells was measured at a wavelength of 570 nm. Cell viability was calculated as a percentage of the viable control cells. All experiments were performed in triplicate. IC_{50} values (the drug concentrations that reduced the number of viable cells to 50% of the control level) were determined from the dose–response curves.

4.6. Flow cytometry

K562 cells (5×10^5 cells/ml) were incubated with test compounds for 24 h. After incubation, cells were centrifuged, washed in PBS and split into two subsamples for viability and cell cycle analysis as described previously [17,19]. For viability analyses, the cells were directly stained with propidium iodide and the percentage of viable cells (*i.e.* those excluding propidium iodide) was determined by flow cytometry using a 488 nm laser (Cell Lab Quanta SC, Beckman Coulter). For cell cycle analysis, the washed cells were fixed with 70% ethanol, washed, stained with propidium iodide and analyzed by flow cytometry using a 488 nm laser (Cell Lab Quanta SC, Beckman Coulter). The sub-diploid fraction was designated as apoptotic.

4.7. Kinase inhibition assay

Kinase assays were performed according to established protocols [17,19]. Briefly, CDK2/cyclin E and Abl kinases were produced in Sf9 insect cells and purified on a NiNTA column (Qiagen). CK2α1 was purchased from ProQinase. CDK2 was assayed with 1 mg/ml histone H1 in the presence of 15 μM ATP, 0.05 μCi [γ-^{33}P]ATP and of the test compound in a final volume of 10 μL, all in a reaction buffer (60 mM HEPES-NaOH, pH 7.5, 3 mM $MgCl_2$, 3 mM $MnCl_2$, 3 μM Na-orthovanadate, 1.2 mM DTT, 2.5 μg/50 μl $PEG_{20.000}$). CK2α1 was assayed in the same buffer but with casein as a substrate (0.2 mg/ml). Abl was assayed with 500 μM of a synthetic peptide (GGEAIYAAPFKK) 10 μM of [γ-^{33}P]ATP and the appropriate quantity of the test compound in a final volume of 10 μL, all in a reaction buffer (25 mM Tris, pH 7.5, 5 mM $MgCl_2$, 0.5 mM EGTA, 1 mM DTT, 0.01% Brij35). The reactions were stopped by adding 5 μL of 3% aq. H_3PO_4. Aliquots were spotted onto P-81 phosphocellulose (Whatman), washed 3× with 0.5% aq. H_3PO_4 and finally air-dried. Kinase inhibition was quantified using a FLA-7000 digital image analyzer (Fujifilm). The concentration of the test compounds required to decrease the kinase activity by 50% was determined from dose–response curves and identified as the IC_{50}.

4.8. Immunoblotting

Immunoblotting analyses were performed as in our previous works [16–19]. Specific antibodies were purchased from Sigma–Aldrich (anti-α-tubulin and peroxidase-labelled secondary antibodies) and Cell Signaling Technology (STAT5, STAT5 phosphorylated at Y694, CrkL phosphorylated at Y207), and Millipore (anti-phosphotyrosine 4G10). Briefly, cellular lysates were prepared by harvesting cells in Laemmli sample buffer. Proteins were separated on SDS-polyacrylamide gels and electroblotted onto nitrocellulose membranes. After blocking, the membranes were incubated with specific primary antibodies overnight, washed and then incubated with peroxidase-conjugated secondary antibodies. Finally, peroxidase activity was detected with ECL+ reagents (AP Biotech) using a CCD camera LAS-4000 (Fujifilm).

4.9. Molecular modelling

3D structures of the studied compounds were prepared using Marvin 5.10.3, 2012, ChemAxon (http://www.chemaxon.com). The crystal structures of CDK2 with NU6102 (PDBID: 2c6o) and Abl with PD180970 (PDBID: 2hzi) were used as the protein docking templates. Polar hydrogens were added to all ligands and proteins with the AutoDock Tools program [27]. Molecular docking was

performed using the AutoDock Vina program [28] with a grid box centred on the protein's active site and a box size of 14 Å. The value of the exhaustiveness parameter was set to 20 (default 8). The two crystal-like poses with the lowest energies were selected for further analysis.

Acknowledgements

This research was funded by the National Science Centre, Poland (grant NN405 092340), the Czech Science Foundation (grant P305/12/0783), the Centre of the Region Haná for Biotechnological Agricultural Research (grant no. ED0007/01/01), Palacky University (Student Project PrF_2014_023), the Operational Program Research and Development for Innovations – European Regional Development Fund (CZ.1.05/2.1.00/03.0058). The authors are grateful to Prof. Robert Kawęcki and Dr. Konrad Zdanowski (Siedlce University of Natural Sciences and Humanities) for providing NMR spectra and Prof. W.T. Miller (Stony Brook University, NY) for providing the Abl construct.

Appendix A. Supplementary data

Supplementary data related to this article can be found at http://dx.doi.org/10.1016/j.ejmech.2014.03.054.

References

[1] J. Zhang, P.L. Yang, N.S. Gray, Nature Reviews Cancer 9 (2009) 28–39.
[2] S. Lapena, A. Giordano, Nature Reviews Drug Discovery 8 (2009) 547–566.
[3] A. Levitzki, Annual Review of Pharmacology and Toxicology 53 (2013) 161–185.
[4] R. Capdeville, E. Buchdunger, J. Zimmermann, A. Matter, Nature Reviews Drug Discovery 1 (2002) 493–502.
[5] A. Quintás-Cardama, H. Kantarjian, J. Cortes, Nature Reviews Drug Discovery 6 (2007) 834–848.
[6] H.J. Lindner, G. Schaden, Chemische Berichte 105 (1972) 1949–1955.
[7] K. Hirata, H. Nakagami, J. Takashina, T. Mahmud, M. Kobayashi, Y. In, T. Ishida, K. Miyamoto, Heterocycles 43 (1996) 1513–1519.
[8] V.V. Smirnov, E.A. Kiprianova, A.D. Garagulya, S.E. Esipov, S.A. Dovjenko, FEMS Microbiology Letters 153 (1997) 357–361.
[9] V. Galasso, Chemical Physics Letters 472 (2009) 237–242.
[10] T.R. Kelly, E.L. Elliott, R. Lebedev, J. Pagalday, Journal of the American Chemical Society 128 (2006) 5646–5647.
[11] T. Gucky, I. Frysova, J. Slouka, M. Hajduch, P. Dzubak, European Journal of Medicinal Chemistry 44 (2009) 891–900.
[12] M. Legraverend, D.S. Grierson, Bioorganic & Medicinal Chemistry 14 (2006) 3987–4006.
[13] R. Jorda, K. Paruch, V. Krystof, Current Pharmaceutical Design 18 (2012) 2974–2980.
[14] V. Krystof, S. Uldrijan, Current Drug Targets 11 (2010) 291–302.
[15] V. Krystof, R. Lenobel, L. Havlicek, M. Kuzma, M. Strnad, Bioorganic & Medicinal Chemistry Letters 12 (2002) 3283–3286.
[16] V. Krystof, I.W. McNae, M.D. Walkinshaw, P.M. Fischer, P. Muller, B. Vojtesek, M. Orsag, L. Havlicek, M. Strnad, Cellular and Molecular Life Sciences 62 (2005) 1763–1771.
[17] M. Zatloukal, R. Jorda, T. Gucky, E. Reznickova, J. Voller, T. Pospisil, V. Malinkova, H. Adamcova, V. Krystof, M. Strnad, European Journal of Medicinal Chemistry 61 (2013) 61–72.
[18] L. Havlicek, K. Fuksova, V. Krystof, M. Orsag, B. Vojtesek, M. Strnad, Bioorganic & Medicinal Chemistry 13 (2005) 5399–5407.
[19] R. Jorda, L. Havlicek, I.W. McNae, M.D. Walkinshaw, J. Voller, A. Sturc, J. Navratilová, M. Kuzma, M. Mistrik, J. Bartek, M. Strnad, V. Kryštof, Journal of Medicinal Chemistry 54 (2011) 2980–2993.
[20] M. Mojzych, A. Rykowski, Heterocycles 53 (2000) 2175–2181.
[21] M. Mojzych, A. Rykowski, Journal of Heterocyclic Chemistry 44 (2007) 1003–1007.
[22] T. Gucky, E. Reznicková, P. Dzubak, M. Hajduch, V. Krystof, Monatshefte für Chemie 141 (2010) 709–714.
[23] J. Carmichael, W. Degraff, A. Gazdar, J. Minna, J. Mitchell, Cancer Research 47 (1987) 936–942.
[24] S.W. Cowan-Jacob, G. Zendrich, A. Floersheimer, P. Furet, J. Liebetanz, G. Rummel, P. Rheinberger, M. Centeleghe, D. Fabbro, P.W. Manley, Acta Crystallographica Section D: Biological Crystallography 63 (2007) 80–93.
[25] I.R. Hardcastle, C.E. Arris, J. Bentley, F.T. Boyle, Y. Chen, N.J. Curtin, J.A. Endicott, A.E. Gibson, B.T. Golding, R.J. Griffin, P. Jewsbury, J. Menyerol, V. Mesguiche, D.R. Newell, M.E. Noble, D.J. Pratt, L.Z. Wang, H.J. Whitfield, Journal of Medicinal Chemistry 47 (2004) 3710–3722.
[26] A. Jacquel, M. Herrant, L. Legros, N. Belhacene, F. Luciano, G. Pages, P. Hofman, P. Auberger, FASEB Journal 17 (2003) 2160–2162.
[27] M.F. Sanner, Journal of Molecular Graphics and Modelling 17 (1999) 57–61.
[28] O. Trott, A.J. Olson, Journal of Computational Chemistry 31 (2010) 455–461.